Inorganic Chemistry

Article

pubs.acs.org/IC

Efficient Visible to Near-UV Photochemical Upconversion Sensitized by a Long Lifetime Cu(I) MLCT Complex

Catherine E. McCusker and Felix N. Castellano*

Department of Chemistry, North Carolina State University, 2620 Yarbrough Drive, Raleigh, North Carolina 27695, United States

Supporting Information

ABSTRACT: The current investigation compares the photochemical upconversion sensitization properties of two long lifetime Cu(I) metal-to-ligand charge transfer (MLCT) chromophores to 3 distinct anthryl-based triplet acceptors. The sensitizers $[Cu(dsbtmp)_2](PF_6)$ (**1**, dsbtmp = 2,9-di(*sec*-butyl)-3,4,7,8-tetramethyl-1,10-phenanthroline) and $[Cu(dsbp)_2](PF_6)$ (**2**, dsbp = 2,9-di(*sec*-butyl-1,10-phenanthroline) were selectively excited in the presence of anthracene, 9,10-diphenylanthracene (DPA), and 9,10-dimethylanthracene (DMA) in degassed dichloromethane solutions. In all instances, triplet energy transfer was observed from selective excitation of the Cu(I) MLCT chromophore to each respective anthryl species. The bimolecular triplet−triplet energy transfer quenching rate constants were extracted from dynamic Stern−Volmer analyses in each case, yielding values below the diffusion limit in dichloromethane. However, the Stern−Volmer quenching constants (K_{SV}'s) were sizable enough (up to ~2300 M^{-1} with **1** as a sensitizer) to support efficient photochemical upconversion. As such, visible to near-UV photochemical upconversion was observed in every instance, along with the anticipated quadratic-to-linear incident light power dependence when pumping at 488 nm. The latter verified that it is indeed sensitized triplet−triplet annihilation responsible for the generation of the anthryl-based singlet fluorescence. Photochemical upconversion quantum efficiencies were evaluated using a relative actinometric method as both a function of incident light power density as well as anthryl acceptor/annihilator concentration. When **1** was used as the sensitizer, upconversion quantum yields as large as 9.2% and 17.8% were observed for DMA and DPA, respectively. Finally, the combination of **1** with DMA was shown to be quite robust, showing no obvious signs of decomposition during 12 h of continuous 488 nm photolysis.

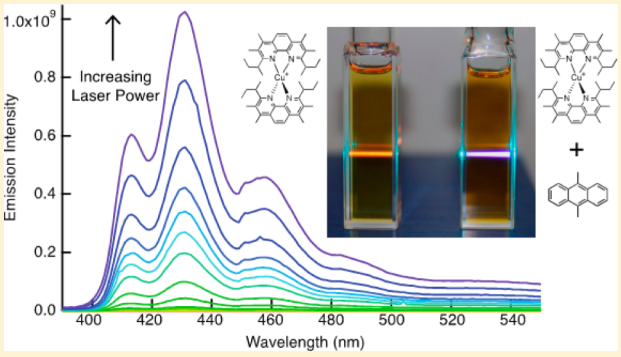

INTRODUCTION

Upconversion photochemistry based on sensitized triplet−triplet annihilation represents a regenerative means to generate high-energy emission from low-energy excitation.[1] Simply stated, a photosensitizer with a high intersystem crossing (ISC) yield is used to sensitize the triplet state of an acceptor through triplet−triplet energy transfer (TTET). When two excited triplet acceptors collide, they can undergo triplet−triplet annihilation (TTA) to form one highly energized singlet acceptor. The singlet acceptor can then return to the ground state through radiative decay, fluorescing at a higher energy than the sensitizer originally absorbed (Figure 1). The phenomenon of sensitized triplet−triplet annihilation was first investigated in the 1960s by Parker and Hatchard, but was inefficient because organic sensitizers with low ISC yields were originally used and the excitation/detection sources were inadequate for routine investigations of this phenomenon.[2−5] Recent advances in the world of photochemical upconversion exploit the use of second and third row transition metal complex sensitizers featuring metal-to-ligand charge transfer (MLCT) excited states or metalloporphyrins/phthalocyanines taking advantage of their internal heavy atom effect enabling ISC yields at or approaching unity, ultimately leading to facile visualization of light-producing upconversion processes.[6−22]

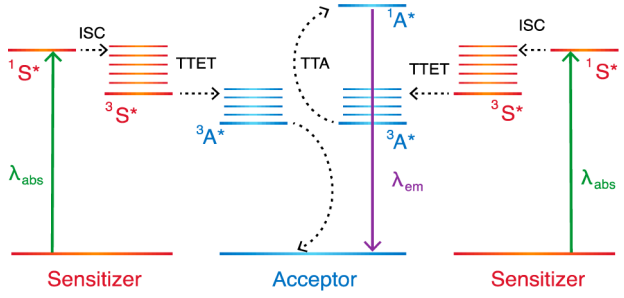

Figure 1. Generalized Jablonski diagram showing the relevant processes in sensitized photon upconversion (ISC = intersystem crossing, TTET = triplet−triplet energy transfer, TTA = triplet−triplet annihilation). Note that two absorbed photons are necessary to generate one emitted photon in this scenario.

Received: April 22, 2015
Published: June 2, 2015

DOI: 10.1021/acs.inorgchem.5b00907
Inorg. Chem. 2015, 54, 6035−6042

Some of the more promising applications of sensitized photon upconversion include solar energy applications such as improving the red photocurrent response of single junction solar cells,[23−30] sensitizing solar fuels photochemistry,[31−34] and solar-based water detoxification[35] in addition to biological and medical applications such as anti-Stokes fluorescence imaging,[36,37] photodynamic therapy,[38] and oxygen sensing.[39] Across these types of applications it is desirable to replace the rare second and third row transition-metal-based photosensitizers with earth abundant alternatives. Unfortunately, there are only a handful of examples of first row metal complexes[40−43] or organic sensitizers[44−48] that have been successfully employed in sensitized photon upconversion schemes.

Copper(I) bis-phenanthroline complexes offer a promising alternative to sensitizers derived from the more rare platinum, palladium, and ruthenium. They have similar light absorption properties with respect to benchmark MLCT chromophore $[Ru(bpy)_3]^{2+}$, and their d^{10} electronic configuration eliminates any low-lying ligand field states that typically deactivate other first row transition metal complexes. Previous work from our laboratory has shown that $[Cu(dpp)_2](PF_6)$ (dpp = 2,9-diphenyl-1,10-phenanthroline) can indeed sensitize photon upconversion, but the process is limited by the inherently short (τ = 250 ns) sensitizer lifetime and high acceptor concentrations required for adequate performance.[42] The photophysical properties of $[Cu(dpp)_2]^+$ and related copper(I) bis-phenanthroline complexes have been extensively investigated for more than 30 years.[49−53] In the ground state, the Cu(I) center prefers a pseudotetrahedral (D_{2d}) geometry. In the MLCT excited state, the copper center is formally oxidized to Cu(II) and therefore undergoes a pseudo-Jahn−Teller distortion. This excited state distortion leads to shortened excited state lifetimes and energy wasting large pseudo-Stokes shifts, which are not ideal for bimolecular triplet energy transfer sensitization. Sterically bulky substituents in the 2,9-positions have been shown to restrict this distortion and lengthen the excited state lifetime. Moreover, methyl groups in the 3,8-positions have been shown to cooperatively enhance the steric hindrance influence of the 2,9-substituents.[54,55] Previously, we have shown that 1,10-phenanthroline ligands with the combination of *sec*-butyl groups in the 2,9-positions and methyl groups in the 3,4,7,8-positions result in a copper(I) bis-phenanthroline complex that possesses an extremely long-lived MLCT excited state (2.8 μs in dichloromethane) even in donor solvents including acetonitrile (τ = 1.5 μs) and methanol (τ = 1.7 μs).[56] This Cu(I) species was later shown to exhibit unprecedented stability over several days when used as a visible light-harvesting sensitizer in a H_2-producing photocatalytic scheme.[57]

The current investigation compares key photochemical upconversion performance metrics of the long-lived $[Cu(dsbtmp)_2](PF_6)$ (**1**) (dsbtmp = 2,9-di(*sec*-butyl)-3,4,7,8-tetramethyl-1,10-phenanthroline) species with the energetically similar $[Cu(dsbp)_2](PF_6)$ (**2**) (dsbp = 2,9-di(*sec*-butyl-1,10-phenanthroline) chromophore (Chart 1), which has a prototypical 400 ns Cu(I) MLCT excited state lifetime. The bimolecular quenching constants, photon upconversion power dependence, and upconversion quantum yields of **1** with a series of acceptors in the anthracene family were evaluated and directly compared to those of **2**. Improvements in the sensitizer excited state lifetime in **1** translated to marked improvement in bimolecular quenching efficiencies and ultimately led to significant increases in upconversion quantum yields with respect to **2** and the previously reported $[Cu(dpp)_2]^+$.

Chart 1. Sensitizers and Acceptors/Annihilators Used in This Study

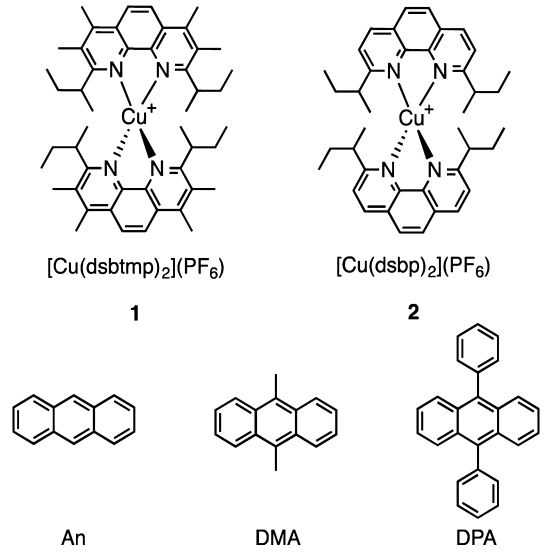

RESULTS AND DISCUSSION

The absorption and photoluminescence spectra of **1** and **2** are presented in Figure 2a. Both complexes have the same characteristic, broad MLCT absorption in the visible, with **1** slightly blue-shifted due to the additional electron donating methyl substituents on the phenanthroline rings. Both complexes also possess red photoluminescence emission, centered at 630 nm in **1** and 690 nm in **2**, which is a superposition of phosphorescence from the lowest ^{3}MLCT state and E-type delayed fluorescence from the close lying ^{1}MLCT state.[56,58] The significant difference in emission energy between **1** and **2** partially reflects the reduced excited state pseudo-Jahn−Teller distortion in **1**, which was the subject of a recently published ultrafast transient absorption study.[53] This reduced distortion ultimately leads to **1** having a much longer excited state lifetime than **2** in dichloromethane solution (2.8 μs vs 400 ns).[56]

Bimolecular Quenching Kinetics. Members of the anthracene family have been shown to effectively quench the excited states of several copper bis-phenanthroline complexes.[59−61] They have also been successfully exploited in photon upconversion systems with energetically similar $[Ru(bpy)_3]^{2+}$ complexes.[6,7,17,62] For these reasons, the bimolecular quenching efficiency of **1** was examined with three distinct acceptors in the anthracene family, anthracene (An), 9,10-dimethylanthracene (DMA), and 9,10-diphenylanthracene (DPA), whose absorption and fluorescence spectra are presented in Figure 2b. DPA is one of the most commonly used acceptors in upconversion photochemistry due to its high-energy fluorescence and near unity singlet fluorescence quantum yield.[9,17,63−70] DMA and An have been used previously in upconversion systems but are less commonly utilized with respect to DPA.[6,7,62,71,72] DMA has an emission energy and quantum yield similar to those of DPA, but is susceptible to exciplex formation at high concentrations. The emission of An is higher energy than either DPA or DMA, but suffers from a low fluorescence quantum yield (Φ_F = 0.3).[73] As

DOI: 10.1021/acs.inorgchem.5b00907
Inorg. Chem. 2015, 54, 6035−6042

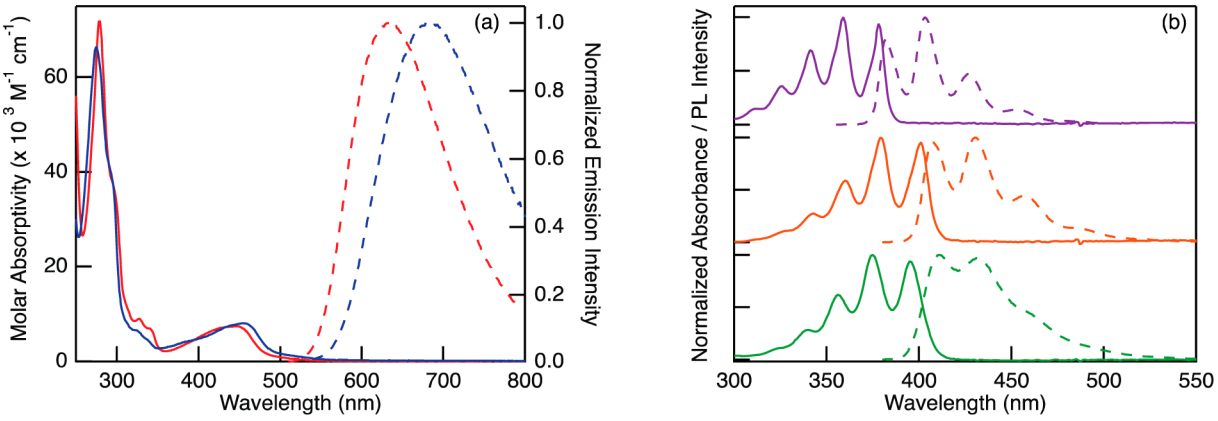

Figure 2. (a) Absorption (solid lines) and normalized photoluminescence (dashed lines) spectra of **1** (red) and **2** (blue) in dichloromethane solution. (b) Normalized absorption (solid lines) and singlet fluorescence (dashed lines) spectra of An (purple), DMA (orange), and DPA (green) in dichloromethane solution.

Table 1. Performance Metrics of Sensitized Photon Upconversion Compositions

sensitizer	acceptor	K_{sv} (M^{-1})	k_q ($\times 10^8$ M^{-1} s^{-1})	λ_{ex} (nm)	λ_{em}[a] (nm)	Φ_{UC}[b] (%)	ΔE[c] (eV)
1	An	2270	9.75	488	384	0.91 ± 0.08 (4 mM)	0.69
	DMA	2060	7.36	488	410	9.2 ± 0.4 (4.4 mM)	0.48
	DPA	1030	4.23	488	414	17.8 ± 0.7 (9 mM)	0.45
2	An	160	4.56	488	404	0.67 ± 0.09 (55 mM)	0.53

[a]Highest energy maximum in the corrected emission spectra. [b]Reported values are the average of at least three independent measurements, and error bars are the standard deviation of those measurements. Acceptor concentrations used are given in parentheses. [c]Energy difference between excitation and upconverted emission ($E_{em} - E_{ex}$).

a point of comparison, the bimolecular quenching and photon upconversion efficiency of **2** were also measured with An. At the high concentrations of DMA and DPA needed for significant quenching of **2**, selective excitation of this Cu(I) sensitizer at 488 nm was no longer possible making it difficult to quantify the upconversion efficiency in those compositions. Therefore, we do not report any upconversion efficiencies of **2** using DMA or DPA acceptors.

$$\frac{\tau_0}{\tau} = 1 + K_{SV}[Q] \quad (1)$$

The Stern–Volmer constants (K_{SV}'s) and the bimolecular quenching constants (k_q's) were obtained for the various donor/acceptor combinations according to the dynamic Stern–Volmer relation, shown in eq 1, where τ_0 and τ are the sensitizer lifetimes in the absence or presence of the quencher, respectively, K_{SV} is the Stern–Volmer constant, $K_{SV} = k_q\tau_0$, and [Q] is the molar concentration of quencher. The K_{SV} and k_q for **1** and **2** with the selected energy acceptors are collected in Table 1. Complex **1** shows moderate quenching behavior with An, DMA, and DPA, with K_{SV} values ranging from 2270 to 1030 M^{-1} and k_q values ranging from 9.75×10^8 to 4.23×10^8 M^{-1} s^{-1}. These values are in the range of those reported for the quenching of $[Ru(dmb)_3]^{2+}$ (dmb = 4,4′-dimethyl-2,2′-bipyridine) with An, DMA, and DPA.[7,62] While these values are small in comparison to values reported for the longer lived Pd(II) porphyrins,[72] they are large enough that >90% quenching of the sensitizer can be achieved with millimolar concentrations of the acceptors. In addition to dynamic quenching, **1** also displays evidence of static quenching by anthracene as evidenced by the small decrease in initial amplitude in the time-resolved emission decays (Supporting Information Figure S1).[74] Stern–Volmer analysis using steady state emission intensities, Supporting Information Figure S3, also results in a linear plot. This plot illustrates that the static quenching is not a significant contribution to the overall quenching of **1** by An, and was therefore not investigated further. None of the other combinations of sensitizers and acceptors showed any evidence for static quenching.

A comparison between the quenching of **1** and **2** by An exemplifies the advantage of using a long-lived Cu(I) MLCT photosensitizer. While there is roughly a 2-fold decrease in the quenching rate constant, most likely due to the lower triplet energy in **2**, the major difference between the two sensitizers is the more than 10-fold difference in the Stern–Volmer quenching constant. This is clearly a result of the difference in excited state lifetimes between **1** and **2** mandating a 10-fold higher An concentration required to quench the excited state of **2** as compared to **1**.

Incident Light Power Dependence. The population of excited singlet acceptor ($^1A^*$) and therefore the upconverted emission intensity is dependent on two competing kinetic processes, k_t, the first order decay of the acceptor triplet state ($^3A^*$), and $k_{tt}[^3A^*]$, the second order triplet–triplet annihilation of the acceptor triplet state;[75,76] the latter is the process that generates the upconverted photoluminescence. The first order rate constant k_t includes both the intrinsic decay of $^3A^*$ and the pseudo-first-order quenching of the $^3A^*$ state by oxygen. These two competing processes result in two distinct kinetic regimes. In the weak annihilation limit k_t is dominant, which results in the upconverted emission signal having a quadratic dependence on excitation intensity. In the strong annihilation limit, $k_{tt}[^3A^*]$ is dominant which results in the upconverted emission signal having a linear dependence on excitation intensity. The strong annihilation limit is the region where the upconversion quantum efficiency is maximized, and the excitation power required to reach that limit is a function of sensitizer absorbance and acceptor concentration. High

DOI: 10.1021/acs.inorgchem.5b00907
Inorg. Chem. 2015, 54, 6035–6042

sensitizer absorbance coupled with efficient TTET maximizes the concentration of ^{3}A*, and therefore the rate of TTA. The intermediate region merely represents the range where both processes are contributing near equal amounts to the ^{3}A* excited state decay.

As presented in Figure 3 and Supporting Information Figures S4–S6, the upconverted emission intensity transitions from a quadratic dependence on light intensity at low power density to having a linear dependence on light intensity at high power density for all four compositions. The quadratic region indicates that the upconverted emission does indeed result from a two-photon process, demonstrating that the observed emission is not simply resulting from inadvertent direct excitation of the acceptor species.[77] The linear region is where the upconversion quantum efficiency has reached its maximum value, and TTA is the dominant pathway for ^{3}A* relaxation, occurring under experimental conditions favoring maximum sensitization of ^{3}A* molecules. For all four compositions under investigation here, the transition between the quadratic region and the linear region occurs with excitation power densities near 1 W/cm^2, which is far above solar irradiance at this excitation wavelength, yet remains easily accessible under laboratory conditions.

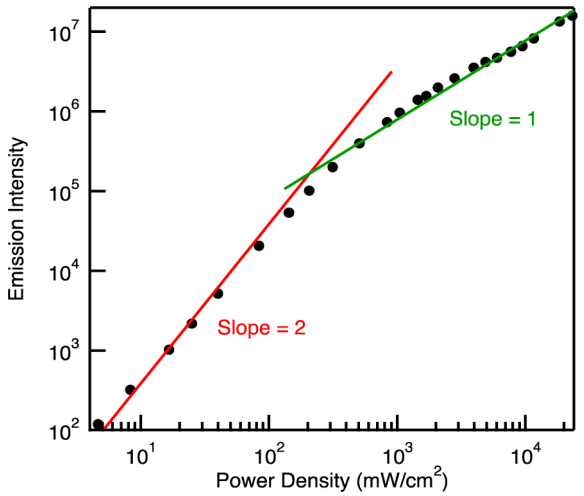

Figure 3. Double logarithmic plot of An emission intensity monitored at 385 nm as a function of 488 nm excitation power density. Solution composition was An (5 mM) sensitized by **1** (0.76 mM) in deoxygenated dichloromethane. Solid lines illustrate a slope of 2 (red, quadratic) and a slope of 1 (green, linear).

Upconversion Quantum Yields. Upconversion quantum yield, the ratio of photons emitted via TTA to absorbed photons, is challenging to measure accurately for a variety of reasons.[29] The nature of the sensitized photon upconversion process requires that the overall quantum efficiency of an upconversion composition will be dependent on the concentrations of the sensitizer and acceptor as well as the excitation power. The upconversion quantum yield (Φ_{UC}) under specified experimental conditions is the product of the quantum yields of each step in the reaction, intersystem crossing (Φ_{ISC}), triplet–triplet energy transfer (Φ_{TTET}), triplet–triplet annihilation (Φ_{TTA}), and acceptor fluorescence (Φ_F) (eq 2).

$$\phi_{UC} = \phi_{ISC} \times \phi_{TTET} \times \phi_{TTA} \times \phi_F \quad (2)$$

Ideally, maximizing the yield of each step should maximize the overall upconversion quantum yield. Unfortunately, these terms cannot be optimized independently, and in some cases maximizing the yield of one step will adversely affect subsequent steps. As discussed above, a higher sensitizer absorbance will result in a higher concentration of ^{3}A*, and therefore more efficient triplet–triplet annihilation resulting in the desired linear power dependence. In the case of the Cu(I) MLCT sensitizers described here, the strong overlap between the absorption spectra of the sensitizers and fluorescence spectra of the acceptors leads to a significant decrease in quantum efficiency with increased sensitizer concentration, Figure 4. The most likely mechanisms result from reabsorption of the upconverted emitted light by the sensitizer as well as favorable Förster energy transfer (spectral overlap) between the ^{1}A* fluorescence spectrum and the sensitizer MLCT absorptions. To best circumvent these processes, upconversion quantum yields were measured for optically dilute solutions of the MLCT sensitizers where the OD ~ 0.2 at the 488 nm excitation wavelength. Even under these circumstances, evidence of the inner-filter effect on the observed upconverted fluorescence spectra in some of the anthryl chromophores is apparent.

The effect of acceptor concentration on overall upconversion yield was also explored using DPA sensitized by **1**. The

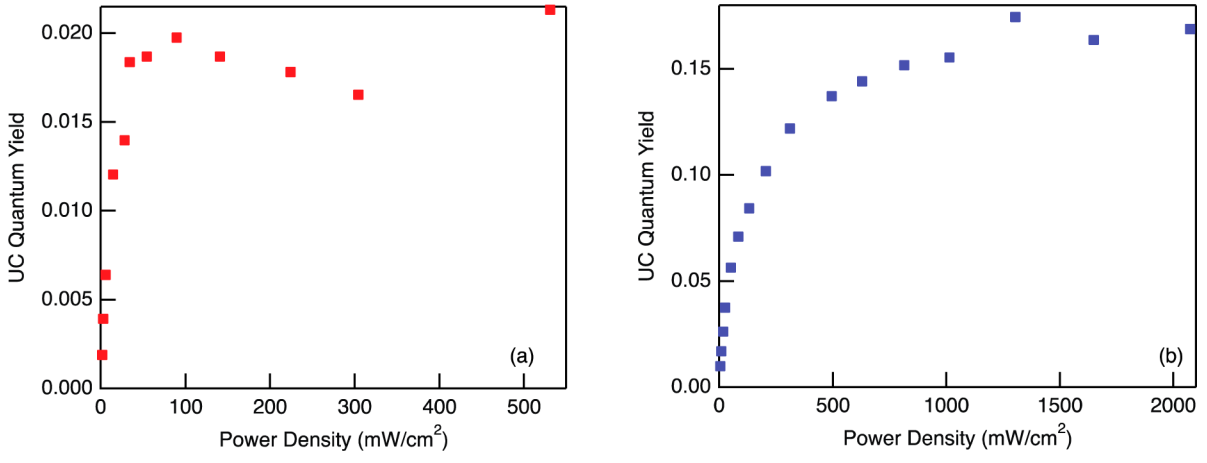

Figure 4. Upconversion quantum yields measured for (a) **1** (0.89 mM) and DPA (8.0 mM) and (b) **1** (0.12 mM) and DPA (8.8 mM) in deoxygenated dichloromethane solutions as a function of excitation power density at 488 nm.

DOI: 10.1021/acs.inorgchem.5b00907
Inorg. Chem. 2015, 54, 6035–6042

upconversion quantum yields of DPA solutions, ranging from 7 to 11 mM, sensitized by **1** (0.12 mM) are presented in Figure 5.

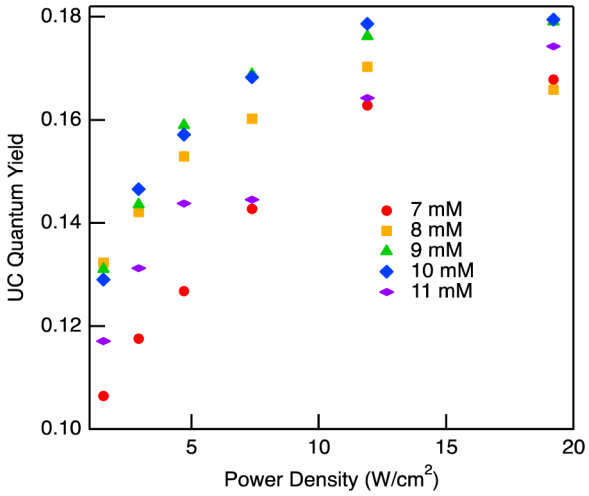

Figure 5. Upconversion quantum yield measured for varying concentrations of DPA sensitized by **1** (0.12 mM) in deoxygenated dichloromethane solution using 488 nm excitation.

The quantum yield is maximized for DPA concentrations of 9–10 mM, which corresponds to ~90% quenching of **1** according to the measured Stern–Volmer constant. The fluorescence quantum yields of anthracene and anthracene derivatives are known to be concentration dependent.[78] At higher concentrations, reabsorption, exciplex formation, and photochemistry can all serve to lower the fluorescence quantum yield of these aromatic acceptors. To aid in the comparison between the various upconversion compositions, the concentrations of all acceptor species were chosen to yield ~90% quenching of the sensitizer in our experiments.

$$\phi_{UC} = 2\phi_{std}\left(\frac{A_{std}}{A_{UC}}\right)\left(\frac{I_{UC}}{I_{std}}\right)\left(\frac{\eta_{UC}}{\eta_{std}}\right)^2 \quad (3)$$

The upconversion quantum yield (Φ_{UC}) of the four compositions was measured relative to $[Ru(bpy)_3](PF_6)_2$ in aerated acetonitrile according to eq 3,[1] where Φ_{std} is the emission quantum yield of the standard, I is the integrated emission intensity of the standard or upconversion solutions, A is the absorbance of the standard and upconversion solutions at 488 nm, and η is the refractive index of the standard and upconversion solvents. Two absorbed photons are needed to generate one emitted photon through TTA; therefore, the factor of 2 is included in eq 3 to make the theoretical maximum quantum yield 1 rather than 0.5. The quantum yield values for the four compositions are reported in Table 1. In a comparison of the quantum yield of An sensitized by **1** (Φ_{UC} = 0.91%) and **2** (Φ_{UC} = 0.67%), the longer-lived **1** shows a ~35% improvement over **2**. Due to the low fluorescence quantum yield of An (Φ_F = 0.3)[73] both An upconversion quantum yields are still less than 1%. Switching from An to the more fluorescent DMA (Φ_F = 0.93)[73] and DPA (Φ_F = 0.91)[73] leads to dramatic improvements in upconversion quantum yield to 9.2% for DMA and 17.8% for DPA (Figure 6). These values are still below the record holding combination of DPA sensitized by Pd(II) octaethylporphyrin (Φ_{UC} = 32%),[31] but they do exceed the reported quantum yields for DMA and DPA sensitized by Ru(II) chromophores (Φ_{UC} = 8–9.8%).[29]

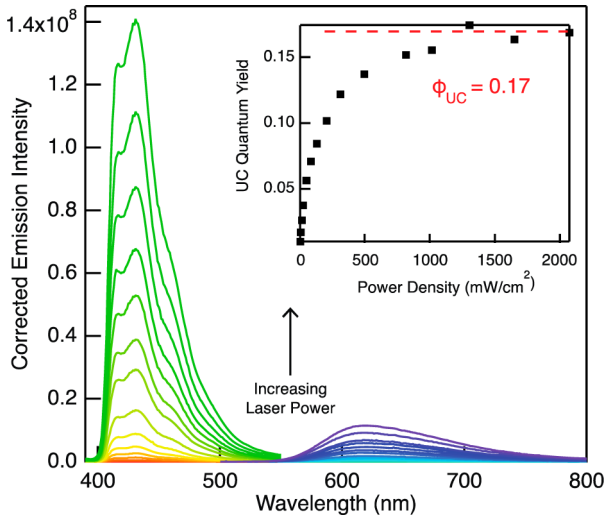

Figure 6. Upconverted emission spectra of DPA (8.9 mM) sensitized by **1** (0.12 mM) in deoxygenated dichloromethane solution and the emission spectra of the $[Ru(bpy)_3](PF_6)_2$ standard in acetonitrile with 488 nm excitation. Inset displays the upconversion quantum yield vs excitation power density. Red dashed line represents the average quantum yield in the plateau region. See text for details.

Comparison between the upconverted emission spectra and the emission spectra of the optically dilute acceptors, Supporting Information Figure S10, shows that for all of the upconversion compositions there is a measurable amount of self-absorption occurring as alluded to in the discussion above. This inner-filter effect, as measured by the mismatch on the blue edge of the fluorescence emission bands, is strongest in the case of An sensitized by **2** due to the much higher An concentration required in that composition.

The photostability of **1** also makes it an ideal probe for investigating the relative stability of DMA and DPA in upconverting compositions. The upconverted emission intensity of DMA and DPA, sensitized by **1**, was monitored as the samples were irradiated at 488 nm (50 mW/cm^2) while stirring for 12 h. As observed in Figure 7, the DMA sample shows almost no change in upconversion intensity over the 12 h of irradiation, whereas the DPA sample intensity decreases significantly over the same period of time. DMA, like An, is known to undergo [4 + 4] photocycloaddition, but unlike An the DMA dimer is unstable and reverts back to the monomer at room temperature resulting in no net chemical change.[79] This result suggests that, even though DPA has a higher upconversion quantum yield and is generally considered to be quite stable, DMA may be the better acceptor choice in applications where long-term photochemical stability is required. At high excitation power density (>10–15 W/cm^2) **1** and **2** did show a slight decrease in the intensity of the MLCT absorption band over time, but at low to moderate excitation powers, the Cu(I) photosensitizers showed no sign of decomposition in any of the upconversion solutions. In all cases the absorbance of the acceptors in the upconversion solutions was too large for accurate measurements; therefore, the change in concentration of the acceptors before and after upconversion could not be directly evaluated. Therefore, the stability and longevity imparted by the DMA acceptors remain under investigation.

DOI: 10.1021/acs.inorgchem.5b00907
Inorg. Chem. 2015, 54, 6035–6042

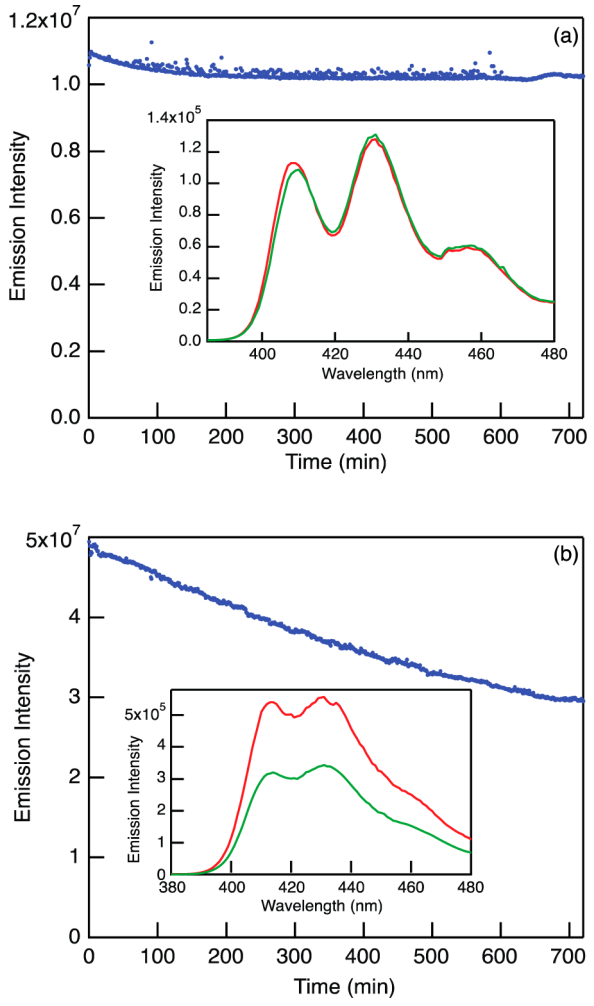

Figure 7. Stability of the upconverted emission intensity, monitored for 12 h while irradiating at 488 nm (50 mW/cm^2). Insets display the upconverted emission spectra before (red) and after (green) 12 h of irradiation. (a) Upconverted emission intensity at 410 nm of DMA (4 mM), sensitized by **1** in deoxygenated dichloromethane solution, and (b) upconverted emission intensity at 415 nm of DPA (8.8 mM), sensitized by **1** in deoxygenated dichloromethane solution.

CONCLUSIONS

The long-lived $[Cu(dsbtmp)_2](PF_6)$ MLCT chromophore is capable of sensitizing photon upconversion through triplet−triplet annihilation in a series of anthracene derivatives, resulting in visible to near-UV wavelength shifting. When the acceptor was DPA or DMA, the measured upconversion quantum yields sensitized by **1** represent marked improvement over the analogous Ru(II) polypyridyl MLCT sensitized systems. Additionally, the upconversion from the DMA-containing composition displayed impressive photostability, with no evidence of decomposition or decrease in emission intensity over 12 h of continuous irradiation. In compositions featuring the $[Cu(dsbtmp)_2]^+$ sensitizer, the upconversion efficiency achieved its maximum value at excitation power densities near 1 W/cm^2 with 488 nm pumping. The design of next generation Cu(I) chromophores with extended lifetimes featuring smaller overlap between the low energy MLCT absorption and the requisite acceptor emission will provide a means to lower the required excitation power density into a range relevant for applications in photochemical upconversion. More importantly, this work provides the necessary proof-of-principle that earth abundant and synthetically facile Cu(I) MLCT complexes can be successfully integrated into upconversion schemes promoting wavelength shifting photochemistry.

EXPERIMENTAL SECTION

General. $[Cu(dsbtmp)_2](PF_6)$[56] and $[Cu(dsbp)_2](PF_6)$[80] were synthesized and purified as previously reported in the literature. Spectrophotometric grade dichloromethane, anthracene (An), 9,10-dimethylanthracene (DMA), and 9,10-diphenylanthracene (DPA) were purchased and used without further purification. Spectroscopic measurements were performed using spectrophotometric grade dichloromethane in 1 cm^2 quartz optical cells. Static absorption spectra were measured with an Agilent 8453 diode array spectrophotometer.

Stern−Volmer Quenching. The Stern−Volmer constants (K_{SV}'s) and the bimolecular quenching constants (k_q's) were obtained according to the dynamic Stern−Volmer relation, $I_0/I = \tau_0/\tau = 1 + K_{SV}[Q]$, where I_0 and I are the sensitizer emission intensities in the absence or presence of the quencher, respectively, and τ_0 and τ are the sensitizer lifetimes in the absence or presence of the quencher, respectively. K_{SV} is the Stern−Volmer constant, $K_{SV} = k_q\tau_0$, and [Q] is the molar concentration of quencher. The slopes of the Stern−Volmer plots were linear over the entire range of measured quencher concentrations. All samples were prepared in a custom 1 cm^2 quartz optical cell with a side arm round-bottom flask and deoxygenated with a minimum of three freeze−pump−thaw cycles. The concentration of sensitizer was chosen to give an absorbance of 0.1−0.2 at the excitation wavelength. Steady state emission spectra were obtained on a FLS920 fluorometer (Edinburgh Instruments). The sample was excited with a 450 W Xe arc lamp, and the emission signal was detected with a Peltier cooled, red sensitive PMT (R2658P Hamamatsu). Time-resolved emission decays were collected with an LP920 laser flash photolysis system (Edinburgh Instruments). The excitation source was the Vibrant 355 LD-UVM Nd:YAG/OPO system (OPOTEK), and data acquisition was controlled by the L900 software program (Edinburgh Instruments). Kinetic traces were collected with a PMT (R928 Hamamatsu) and fit with single exponential decay functions using IGOR Pro.

Power Dependence. Samples were prepared in an inert atmosphere glovebox (MBraun), using spectrophotometric grade dichloromethane, which was previously deoxygenated by at least five freeze−pump−thaw cycles. Solutions were measured in air-free 1 cm^2 quartz optical cells. The concentration of sensitizer was chosen to give an absorbance of ∼1.0 at the excitation wavelength, and the concentration of acceptor was chosen to quench the sensitizer by at least 90%, according to the measured K_{SV}. The 488 nm line of an Ar/Kr ion laser (Innova 70C Coherent), focused to a ∼1.25 mm spot, was used as the excitation source. The excitation power was measured using a Nova II/PD300-UV power meter/detector (Ophir). An appropriate long-pass filter (475 nm) or 488 nm bandpass filter was used to filter the excitation beam to prevent direct excitation of the acceptor, and solutions of the acceptors alone showed no emission. Emission intensities at the highest energy maxima of the upconverted emission (415, 405, or 385 ± 5 nm) were recorded over 1 min in time-based mode with the FLS920 fluorometer described above. For higher excitation powers, the use of neutral density filters before the detector was necessary to prevent PMT saturation. The final emission intensities in these samples were corrected for the filter transmittance. The average emission intensities were plotted versus the measured excitation power density. The slope of the plot on a double logarithmic scale was used to differentiate the quadratic (slope = 2) and linear (slope = 1) regions.

Quantum Yield. Upconversion quantum yields were measured relative to $[Ru(bpy)_3](PF_6)_2$ in aerated acetonitrile (Φ_{std} = 0.018[78]). Optically dilute upconversion solutions were prepared in an inert atmosphere glovebox in spectrophotometric grade dichloromethane and measured in air-free 1 cm^2 quartz optical cells. In the upconverting

DOI: 10.1021/acs.inorgchem.5b00907
Inorg. Chem. 2015, 54, 6035−6042

solutions, the concentration of sensitizer was chosen to give an absorbance of ~0.2 at 488 nm, approximately 0.15 mM for **1** and 0.08 mM for **2**, and the acceptor concentration was chosen to give at least 90% sensitizer quenching according to the measured K_{SV} values. Samples were excited with the 488 nm line of the Ar/Kr ion laser, and the emission spectra were collected with the FLS920 fluorometer as described above. An appropriate long-pass filter (475 nm) or 488 nm bandpass filter was used to filter the excitation beam to prevent direct excitation of the acceptor. The excitation power was varied, and the upconversion quantum yield (Φ_{uc}) at each power was calculated using eq 3.[1] The quantum yield values reported in Table 1 are the average of three independent measurements.

■ ASSOCIATED CONTENT

Supporting Information

Stern−Volmer plots, power dependence measurements, and upconversion quantum yield data. The Supporting Information is available free of charge on the ACS Publications website at DOI: 10.1021/acs.inorgchem.5b00907.

■ AUTHOR INFORMATION

Corresponding Author

*E-mail: fncastel@ncsu.edu.

Author Contributions

The manuscript was written through contributions of both authors. Both authors have given approval to the final version of the manuscript.

Notes

The authors declare no competing financial interest.

■ ACKNOWLEDGMENTS

This material is based upon work supported by the U.S. Department of Energy, Office of Science, Office of Basic Energy Sciences, under Award Number DE-SC0011979.

■ REFERENCES

(1) Singh-Rachford, T. N.; Castellano, F. N. *Coord. Chem. Rev.* **2010**, *254*, 2560−2573.
(2) Parker, C. A.; Hatchard, C. G. *Proc. R. Soc. A* **1962**, *269*, 574−584.
(3) Parker, C. A.; Hatchard, C. G. *Proc. Chem. Soc., London* **1962**, 386−387.
(4) Parker, C. A. *Proc. R. Soc. A* **1963**, *276*, 125−135.
(5) Parker, C. A.; Hatchard, C. G.; Joyce, T. A. *J. Mol. Spectrosc.* **1964**, *14*, 311−319.
(6) Kozlov, D. V.; Castellano, F. N. *Chem. Commun.* **2004**, 2860−2861.
(7) Islangulov, R. R.; Kozlov, D. V.; Castellano, F. N. *Chem. Commun.* **2005**, 3776−3778.
(8) Zhao, W.; Castellano, F. N. *J. Phys. Chem. A* **2006**, *110*, 11440−11445.
(9) Islangulov, R. R.; Lott, J.; Weder, C.; Castellano, F. N. *J. Am. Chem. Soc.* **2007**, *129*, 12652−12653.
(10) Baluschev, S.; Yakutkin, V.; Miteva, T.; Wegner, G.; Roberts, T.; Nelles, G.; Yasuda, A.; Chernov, S.; Aleshchenkov, S.; Cheprakov, A. *New J. Phys.* **2008**, *10*, 013007.
(11) Singh-Rachford, T. N.; Castellano, F. N. *J. Phys. Chem. C* **2008**, *112*, 3550−3556.
(12) Singh-Rachford, T. N.; Haefele, A.; Ziessel, R.; Castellano, F. N. *J. Am. Chem. Soc.* **2008**, *130*, 16164−16165.
(13) Singh-Rachford, T. N.; Nayak, A.; Muro-Small, M. L.; Goeb, S.; Therien, M. J.; Castellano, F. N. *J. Am. Chem. Soc.* **2010**, *132*, 14203−14211.
(14) Cheng, Y. Y.; Fückel, B.; Khoury, T.; Clady, R. G.; Ekins-Daukes, N. J.; Crossley, M. J.; Schmidt, T. W. *J. Phys. Chem. A* **2011**, *115*, 1047−1053.
(15) Bergamini, G.; Ceroni, P.; Fabbrizi, P.; Cicchi, S. *Chem. Commun.* **2011**, *47*, 12780−12782.
(16) Ji, S.; Wu, W.; Zhao, J.; Guo, H.; Wu, W. *Eur. J. Inorg. Chem.* **2012**, *2012*, 3183−3190.
(17) Boutin, P. C.; Ghiggino, K. P.; Kelly, T. L.; Steer, R. P. *J. Phys. Chem. Lett.* **2013**, *4*, 4113−4118.
(18) Mani, T.; Vinogradov, S. A. *J. Phys. Chem. Lett.* **2013**, 2799−2804.
(19) Wu, W.; Liu, L.; Cui, X.; Zhang, C.; Zhao, J. *Dalton Trans.* **2013**, *42*, 14374−14379.
(20) El-Ballouli, A. O.; Khnayzer, R. S.; Khalife, J. C.; Fonari, A.; Hallal, K. M.; Timofeeva, T. V.; Patra, D.; Castellano, F. N.; Wex, B.; Kaafarani, B. R. *J. Photochem. Photobiol. A* **2013**, *272*, 49−57.
(21) Duan, P.; Yanai, N.; Kimizuka, N. *Chem. Commun.* **2014**, *50*, 13111−13113.
(22) Peng, J.; Jiang, X.; Guo, X.; Zhao, D.; Ma, Y. *Chem. Commun.* **2014**, *50*, 7828−7830.
(23) Atre, A. C.; Dionne, J. A. *J. Appl. Phys.* **2011**, *110*, 034505−034505−9.
(24) de Wild, J.; Meijerink, A.; Rath, J. K.; van Sark, W. G. J. H. M.; Schropp, R. E. I. *Energy Environ. Sci.* **2011**, *4*, 4835.
(25) Cheng, Y. Y.; Fückel, B.; MacQueen, R. W.; Khoury, T.; Clady, R. G. C. R.; Schulze, T. F.; Ekins-Daukes, N. J.; Crossley, M. J.; Stannowski, B.; Lips, K.; Schmidt, T. W. *Energy Environ. Sci.* **2012**, *5*, 6953.
(26) Schulze, T. F.; Cheng, Y. Y.; Fückel, B.; MacQueen, R. W.; Danos, A.; Davis, N. J. L. K.; Tayebjee, M. J. Y.; Khoury, T.; Clady, R. G. C. R.; Ekins-Daukes, N. J.; Crossley, M. J.; Stannowski, B.; Lips, K.; Schmidt, T. W. *Aust. J. Chem.* **2012**, *65*, 480.
(27) Baluschev, S.; Nelles, G.; Landfester, K.; Miteva, T. *Proc. SPIE* **2012**, 84710E.
(28) Nattestad, A.; Cheng, Y. Y.; MacQueen, R. W.; Schulze, T. F.; Thompson, F. W.; Mozer, A. J.; Fückel, B.; Khoury, T.; Crossley, M. J.; Lips, K.; Wallace, G. G.; Schmidt, T. W. *J. Phys. Chem. Lett.* **2013**, *4*, 2073−2078.
(29) Gray, V.; Dzebo, D.; Abrahamsson, M.; Albinsson, B.; Moth-Poulsen, K. *Phys. Chem. Chem. Phys.* **2014**, *16*, 10345−10352.
(30) Schulze, T. F.; Schmidt, T. W. *Energy Environ. Sci.* **2015**, *8*, 103−125.
(31) Khnayzer, R. S.; Blumhoff, J.; Harrington, J. A.; Haefele, A.; Deng, F.; Castellano, F. N. *Chem. Commun.* **2012**, *48*, 209−211.
(32) Börjesson, K.; Dzebo, D.; Albinsson, B.; Moth-Poulsen, K. *J. Mater. Chem. A* **2013**, *1*, 8521.
(33) Wang, B.; Sun, B.; Wang, X.; Ye, C.; Ding, P.; Liang, Z.; Chen, Z.; Tao, X.; Wu, L. *J. Phys. Chem. C* **2014**, *118*, 1417−1425.
(34) Kwon, O. S.; Kim, J. H.; Cho, J. K.; Kim, J. H. *ACS Appl. Mater. Interfaces* **2015**, *7*, 318−325.
(35) Kim, J. H.; Kim, J. H. *J. Am. Chem. Soc.* **2012**, *134*, 17478−17481.
(36) Liu, Q.; Yin, B.; Yang, T.; Yang, Y.; Shen, Z.; Yao, P.; Li, F. *J. Am. Chem. Soc.* **2013**, *135*, 5029−5037.
(37) Wohnhaas, C.; Mailander, V.; Droge, M.; Filatov, M. A.; Busko, D.; Avlasevich, Y.; Baluschev, S.; Miteva, T.; Landfester, K.; Turshatov, A. *Macromol. Biosci.* **2013**, *13*, 1422−1430.
(38) Askes, S. H.; Bahreman, A.; Bonnet, S. *Angew. Chem., Int. Ed.* **2014**, *53*, 1029−1033.
(39) Borisov, S. M.; Larndorfer, C.; Klimant, I. *Adv. Funct. Mater.* **2012**, *22*, 4360−4368.
(40) O'Brien, J. A.; Rallabandi, S.; Tripathy, U.; Paige, M. F.; Steer, R. P. *Chem. Phys. Lett.* **2009**, *475*, 220−222.
(41) Sugunan, S. K.; Tripathy, U.; Brunet, S. M.; Paige, M. F.; Steer, R. P. *J. Phys. Chem. A* **2009**, *113*, 8548−8556.
(42) McCusker, C. E.; Castellano, F. N. *Chem. Commun.* **2013**, *49*, 3537−3539.
(43) Cui, X.; Zhao, J.; Yang, P.; Sun, J. *Chem. Commun.* **2013**, *49*, 10221−10223.
(44) Chen, H. C.; Hung, C. Y.; Wang, K. H.; Chen, H. L.; Fann, W. S.; Chien, F. C.; Chen, P.; Chow, T. J.; Hsu, C. P.; Sun, S. S. *Chem. Commun.* **2009**, 4064−4066.

DOI: 10.1021/acs.inorgchem.5b00907
Inorg. Chem. 2015, 54, 6035−6042

(45) Fückel, B.; Roberts, D. A.; Cheng, Y. Y.; Clady, R. G. C. R.; Piper, R. B.; Ekins-Daukes, N. J.; Crossley, M. J.; Schmidt, T. W. *J. Phys. Chem. Lett.* **2011**, *2*, 966−971.
(46) Wu, W.; Guo, H.; Wu, W.; Ji, S.; Zhao, J. *J. Org. Chem.* **2011**, *76*, 7056−7064.
(47) Wu, W.; Zhao, J.; Sun, J.; Guo, S. *J. Org. Chem.* **2012**, *77*, 5305−5312.
(48) Moor, K.; Kim, J. H.; Snow, S.; Kim, J. H. *Chem. Commun.* **2013**, *49*, 10829−10831.
(49) Armaroli, N.; Accorsi, G.; Cardinali, F.; Listorti, A. *Top. Curr. Chem.* **2007**, *280*, 69−115.
(50) Lavie-Cambot, A.; Cantuel, M.; Leydet, Y.; Jonusauskas, G.; Bassani, D. M.; McClenaghan, N. D. *Coord. Chem. Rev.* **2008**, *252*, 2572−2584.
(51) Iwamura, M.; Takeuchi, S.; Tahara, T. *Acc. Chem. Res.* **2015**, *48*, 782−791.
(52) Mara, M. W.; Fransted, K. A.; Chen, L. X. *Coord. Chem. Rev.* **2015**, *282*−*283*, 2−18.
(53) Garakyaraghi, S.; Danilov, E. O.; McCusker, C. E.; Castellano, F. N. *J. Phys. Chem. A* **2015**, *119*, 3181−3193.
(54) Eggleston, M. K.; McMillin, D. R.; Koenig, K. S.; Pallenberg, A. J. *Inorg. Chem.* **1997**, *36*, 172−176.
(55) Cunningham, C. T.; Cunningham, K. L. H.; Michalec, J. F.; McMillin, D. R. *Inorg. Chem.* **1999**, *38*, 4388−4392.
(56) McCusker, C. E.; Castellano, F. N. *Inorg. Chem.* **2013**, *52*, 8114−8120.
(57) Khnayzer, R. S.; McCusker, C. E.; Olaiya, B. S.; Castellano, F. N. *J. Am. Chem. Soc.* **2013**, *135*, 14068−14070.
(58) Parker, W. L.; Crosby, G. A. *J. Phys. Chem.* **1989**, *93*, 5692−5696.
(59) Castellano, F. N.; Ruthkosky, M.; Meyer, G. J. *Inorg. Chem.* **1995**, *34*, 3−4.
(60) Ruthkosky, M.; Castellano, F. N.; Meyer, G. J. *Inorg. Chem.* **1996**, *35*, 6406−6412.
(61) Leydet, Y.; Bassani, D. M.; Jonusauskas, G.; McClenaghan, N. D. *J. Am. Chem. Soc.* **2007**, *129*, 8688−8689.
(62) Singh-Rachford, T. N.; Islangulov, R. R.; Castellano, F. N. *J. Phys. Chem. A* **2008**, *112*, 3906−3910.
(63) Baluschev, S.; Yakutkin, V.; Wegner, G.; Minch, B.; Miteva, T.; Nelles, G.; Yasuda, A. *J. Appl. Phys.* **2007**, *101*, 023101.
(64) Singh-Rachford, T. N.; Lott, J.; Weder, C.; Castellano, F. N. *J. Am. Chem. Soc.* **2009**, *131*, 12007−12014.
(65) Simon, Y. C.; Bai, S.; Sing, M. K.; Dietsch, H.; Achermann, M.; Weder, C. *Macromol. Rapid Commun.* **2012**, *33*, 498−502.
(66) Monguzzi, A.; Frigoli, M.; Larpent, C.; Tubino, R.; Meinardi, F. *Adv. Funct. Mater.* **2012**, *22*, 139−143.
(67) Cao, X.; Hu, B.; Zhang, P. *J. Phys. Chem. Lett.* **2013**, *4*, 2334−2338.
(68) Poorkazem, K.; Hesketh, A. V.; Kelly, T. L. *J. Phys. Chem. C* **2014**, 140317160829006.
(69) Monguzzi, A.; Meinardi, F. *J. Phys. Chem. A* **2014**, *118*, 1439−1442.
(70) Duan, P.; Yanai, N.; Nagatomi, H.; Kimizuka, N. *J. Am. Chem. Soc.* **2015**, *137*, 1887−1894.
(71) Islangulov, R. R.; Castellano, F. N. *Angew. Chem., Int. Ed.* **2006**, *45*, 5957−5959.
(72) Deng, F.; Blumhoff, J.; Castellano, F. N. *J. Phys. Chem. A* **2013**, *117*, 4412−4419.
(73) Montalti, M.; Credi, A.; Prodi, L.; Gandolfi, M. T. *Handbook of Photochemistry*, 3rd Ed.; CRC Press: Boca Raton, FL, 2006.
(74) Lakowicz, J. R. *Principles of Fluorescence Spectroscopy*; Springer US: Boston, MA, 2006.
(75) Haefele, A.; Blumhoff, J.; Khnayzer, R. S.; Castellano, F. N. *J. Phys. Chem. Lett.* **2012**, *3*, 299−303.
(76) Schmidt, T. W.; Castellano, F. N. *J. Phys. Chem. Lett.* **2014**, *5*, 4062−4072.
(77) Wen, X.; Yu, P.; Toh, Y. R.; Ma, X.; Tang, J. *Chem. Commun.* **2014**, *50*, 4703−4706.
(78) Suzuki, K.; Kobayashi, A.; Kaneko, S.; Takehira, K.; Yoshihara, T.; Ishida, H.; Shiina, Y.; Oishi, S.; Tobita, S. *Phys. Chem. Chem. Phys.* **2009**, *11*, 9850−9860.
(79) Bouas-Laurent, H.; Castellan, A. *Chem. Commun.* **1970**, 1648−1649.
(80) Pallenberg, A. J.; Koenig, K. S.; Barnhart, D. M. *Inorg. Chem.* **1995**, *34*, 2833−2840.

DOI: 10.1021/acs.inorgchem.5b00907
Inorg. Chem. 2015, 54, 6035−6042